J. Inst. Eng. India Ser. B (April 2019) 100(2):153–167
https://doi.org/10.1007/s40031-018-0369-x

ORIGINAL CONTRIBUTION

Impact of TCPS, SMES and DFIG on Load Frequency Control of Nonlinear Power System Using Differential Evolution Algorithm

A. Kumar[1] · **S. Shuhag**[1]

Received: 6 July 2018 / Accepted: 28 November 2018 / Published online: 19 December 2018

Abstract In recent times, wind power is increasingly being integrated in the existing power system network for well-known reasons, but due to unpredictable variations in wind speed, the load frequency control (LFC) of such power systems becomes a difficult task. This paper addresses the problem of LFC of a multi-source hydrothermal nonlinear power system having wind power penetration. Differential evolution (DE) algorithm has been used to optimally tune the proportional, integral and derivative controller used for LFC in the power system subjected to fluctuations of wind power and load. The reheat and generation rate constraints nonlinearities have been considered appropriately for both areas. Besides, the impact of thyristor-controlled phase shifter (TCPS) and superconducting magnetic energy storage (SMES) on the LFC performance has been analyzed with the parameters of TCPS and SMES being tuned using DE algorithm. The system has been investigated for various operating conditions including the weak grid condition to establish the effectiveness of the proposed approach for wide variations in system conditions. The performance is analyzed and discussed in respect of frequency and tie-line power deviations, peak overshoot, settling time, and value of performance index. Further, robustness of the system is investigated by varying the system parameters from − 50 to + 50% in steps of 25% and step load disturbance from 1 to 20% in steps of 5%. Modeling and simulations are carried out using MATLAB/Simulink® to demonstrate the effectiveness of the DE algorithm.

✉ A. Kumar
amitkumar357@nitkkr.ac.in

[1] Electrical Engineering Department, NIT Kurukshetra, Kurukshetra, India

Keywords Load frequency control (LFC) · Differential evolution (DE) · Doubly fed induction generator (DFIG) · Superconducting magnetic energy storage (SMES) · Thyristor-controlled phase shifter (TCPS)

Introduction

Today, the use of wind energy is growing rapidly for electric power generation, but there are difficulties associated with control of power systems having wind power integration due to weather dependency of the wind power. The LFC of such power systems has been attempted and reported in the literature using various control schemes and optimization algorithms. The use of doubly fed induction generator (DFIG)-based wind turbine, as an integrated subsystem of the power system to support the frequency regulation, has been reported [1–8].

As an active power source, the use of SMES, due to its fast dynamics, has been established as the most effective stabilizer for frequency oscillations occurring due to the sudden load changes [9, 10]. Also, the use of TCPS, a flexible AC transmission systems (FACTS) device, has been explored for its use in LFC [11, 12]. It is found in the literature that thermal–thermal or hydrothermal multi-area multi-source power system models are most commonly used for LFC studies but without penetration of wind power [13–15]. Most of these studies have used classical control concepts; however, classical control techniques have their limitations, especially for nonlinear power system models. Many control and optimization techniques such as conventional [16], two fuzzy rules for integral and proportional gains of PI controller [17], genetic algorithm-

based PI and proportional, integral and derivative (PID) controller [18], particle swarm optimization [19, 20], bacterial foraging optimization algorithm [21], hybrid BFOA–PSO algorithm [22], artificial neural network [23], linear-quadratic optimal output feedback controller [24], suboptimal controller [25], generalized neural network approach [26], hybrid gravitational search and pattern search algorithm [27], firefly algorithm-optimized fuzzy PID controller [28], teaching–learning-based optimization [29], hybrid LUS–TLIB-optimized fuzzy PID controller [30] have been proposed for LFC studies of interconnected power systems.

In a large grid, the fluctuations in frequency have little effect on the overall quality of the power, but in a weak grid network, these fluctuations do have a significant impact on the overall quality of the power and therefore must be eliminated. Hence, the frequency regulation in a weak grid system is more challenging than in large grids [31, 32]. For the same reason, with increasing utilization of inertia-less types of generation in power grids, it becomes essential for DFIG, TCPS and SMES to participate in frequency regulation.

In the light of above, this paper implements the DE-based optimal tuning of conventional I/PI/PID controllers for LFC of multi-source hydrothermal power system with and without wind power penetration. Additionally, the effect of TCPS and SMES on the LFC performance is also investigated with the parameters of TCPS and SMES being tuned using DE algorithm. The system has also been investigated for the weak grid condition to establish the effectiveness of the proposed approach for wide variations in system operating conditions. Besides, the sensitivity analysis has also been carried out for robustness study under wide variations in loading pattern and system parameters. Simulations results are presented to show the effectiveness of the implemented algorithm under different operating conditions.

System Description

The following subheads describe the system under study.

Model of Power System

Figure 1 shows the linearized model of the multi-source hydrothermal system used in this study. Hydro- and reheat thermal generating units are represented as in [16]. Also, the DFIG, TCPS and SMES are incorporated in the model as shown. Nominal parameters of the system, used in this study, are given in Appendix. The controller gains are tuned using DE algorithm technique. Integral of time multiplied absolute error (ITAE), given by Eq. (1), is the cost function used for optimization because it has the advantage of giving less settling time and maximum overshoot compared to other cost functions [11].

$$\text{ITAE} = \int (|\Delta f_1| + |\Delta f_2| + |\Delta P_{\text{tie12}}|) \cdot t \cdot \mathrm{d}t \tag{1}$$

Modeling of Tie-Line Power Flow Exchange Considering TCPS in Series with the Tie-Line

The TCPS is connected in series with the tie-line near area 1, as shown in Fig. 2. Resistance of the tie-line is neglected to make the mathematical descriptions and computations simpler.

The speed deviation $\Delta\omega_1$ of area 1 is taken as input signal to the TCPS, and the output signal of the TCPS regulates the tie-line power flow as per the following mathematical description [11].

$$\Delta P_{\text{tie12}}(s) = \Delta P^0_{\text{tie12}}(s) + \Delta P_{\text{TCPS}}(s) \tag{2}$$

where ΔP_{tie12} is tie-line power, $\Delta P^0_{\text{tie12}}$ is the tie-line power in steady state, and ΔP_{TCPS} is the change in power of TCPS which is given by (2)

$$\Delta P_{\text{TCPS}}(s) = T_{12}\frac{K_\varphi}{1+T_{PS}}\Delta\omega_1(s) \tag{3}$$

where T_{12} is tie-line gain, K_φ is stabilization gain, T_{PS} is time constant of TCPS, and $\Delta\omega_1(s)$ is per unit rotor speed deviation.

The transfer function representation of TCPS as a frequency regulator is shown in Fig. 3.

Modeling of SMES

The basic configuration of an SMES is shown in Fig. 4. The use of this device as an active power source is well established. Because of its very fast dynamics, SMES plays very important role in LFC applications as well. The obvious disadvantage is in its practical implementation where extremely low temperature is required to be maintained. The theoretical explanation of the working principle can be referred from [9, 10]; therefore, the description here is avoided. For coordination and control of SMES, the values of the parameters, namely stabilization gain K_{SMES} and time constants T_{SMES}, T_1, T_2, T_3 and T_4, have been adapted from [10]. The transfer function model of the SMES as implemented in this work is shown in Fig. 5.

Modeling of DFIG

DFIG, driven by wind turbine, is capable of generating electric power with variable mechanical speed and participates in frequency regulation as one of the source of active power. Modeling of DFIG from the viewpoint of active

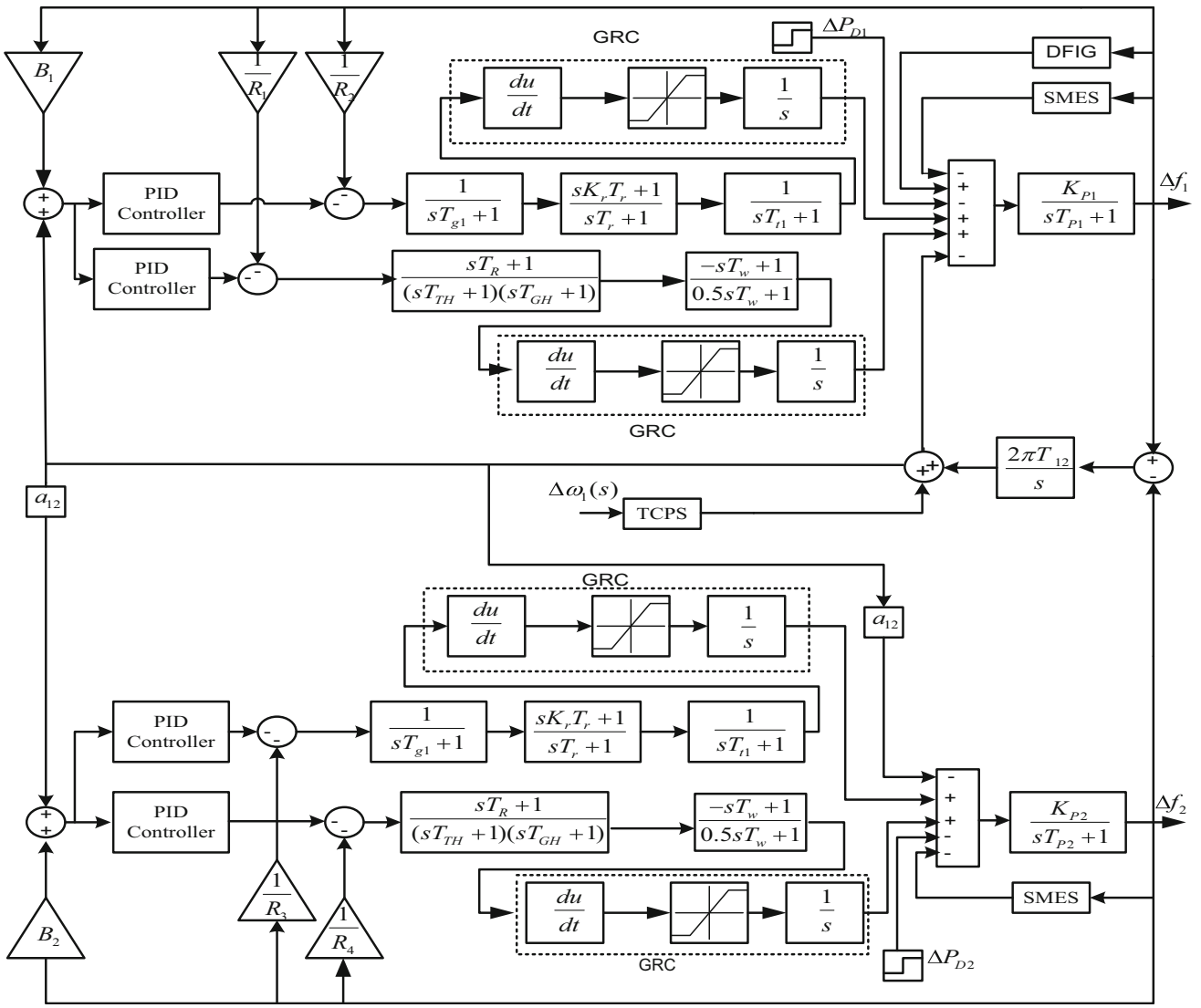

Fig. 1 Block diagram representation of the system

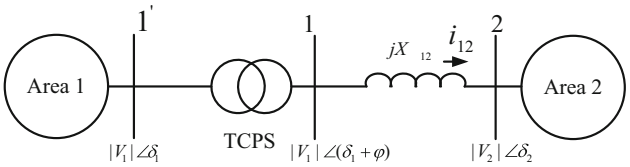

Fig. 2 Configuration of TCPS in power system

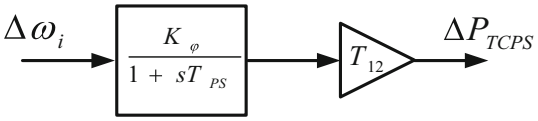

Fig. 3 Block diagram representation showing TCPS as a frequency regulator

power control with dynamic participation of wind turbine is depicted in Fig. 6 which is based on inertial control and is adapted from [5]. The DFIG model and control scheme of Fig. 6 is implemented in MATLAB for simulation purpose in this work.

From Fig. 6, it can be brought that the total active power, ΔP_{NC}, injected by the DFIG is given by:

$$\Delta P_{\mathrm{NC}} = \Delta P_f^* + \Delta P_\omega^* \tag{4}$$

where ΔP_f^* is a function of change in frequency and rate of change of frequency and ΔP_ω^* is a function of optimal turbine speed

The injected active power by the wind turbine during disturbances is compared with $\Delta P_{\mathrm{NCref}}$ for obtaining maximum power output, while maintaining reference rotor speed.

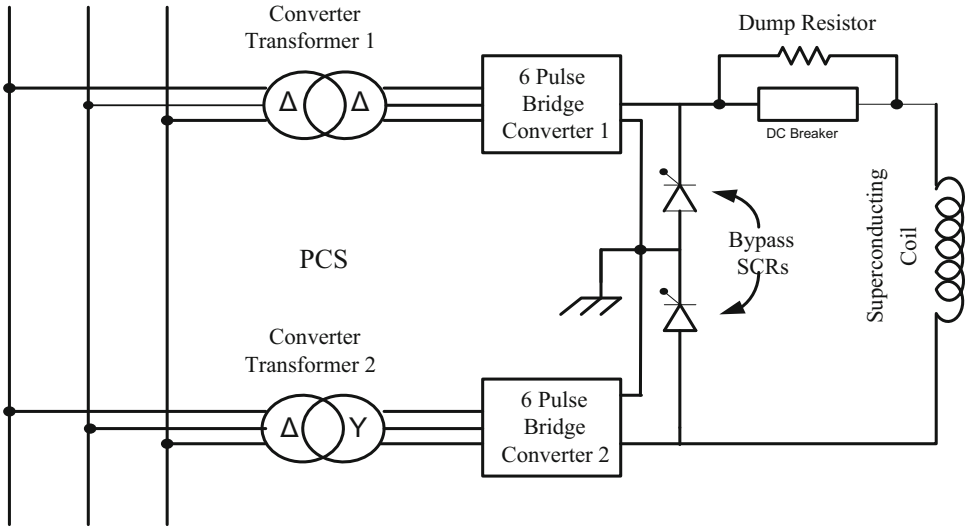

Fig. 4 Configuration of SMES in power system

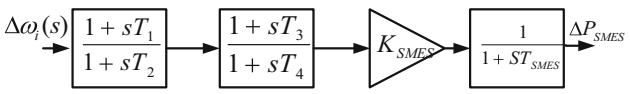

Fig. 5 Transfer function model of SMES as frequency regulator

Control and Optimization Methodology used

The control structures and the optimization scheme used in this work are detailed under the following subheadings.

Control Structure

The standard PID control structure and its variants are used which are capable of providing excellent control performance even under varying operating conditions and/or system parametric variations, provided the controller gain parameters are optimally tuned. The outputs of the controllers are used as control inputs u_i and area control errors e_i to the power system. The transfer function model of the PID controller is expressed as:

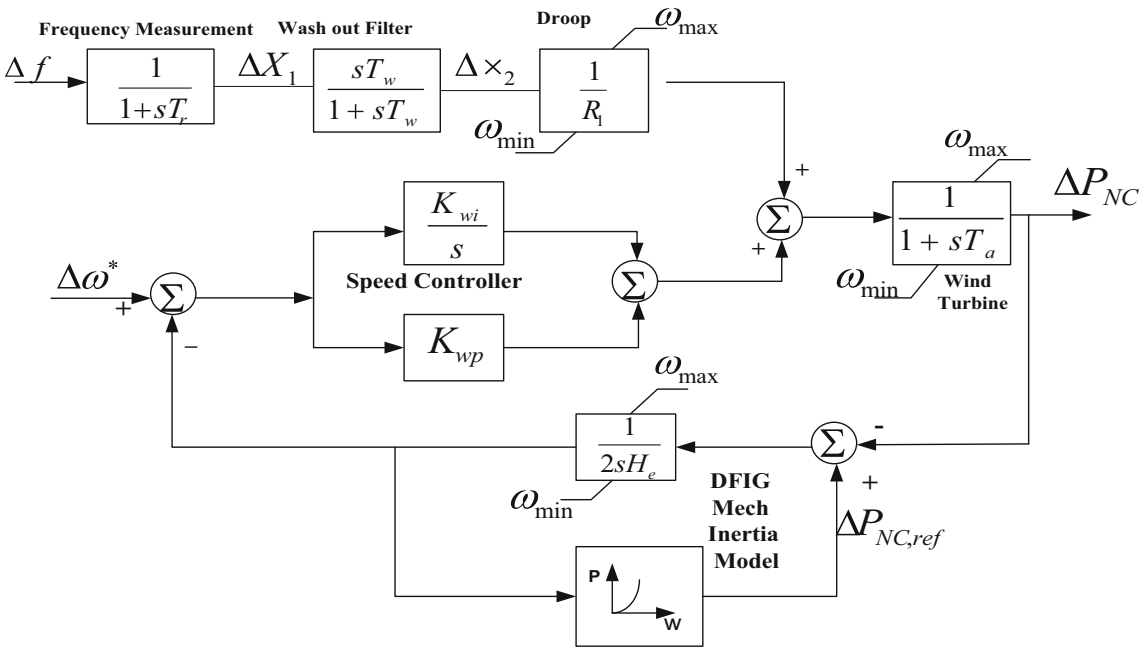

Fig. 6 Model of DFIG-based wind turbine inertial control

$$\mathrm{TF_{PID}} = \left[K_\mathrm{P} + K_\mathrm{I}\left(\frac{1}{s}\right) + K_\mathrm{D}s\right] \quad (5)$$

where K_P, K_I and K_D are the proportional, integral and derivative gains, respectively. The PID controllers in both areas are designed to be nonidentical. The control signal, which is the output of the PID controller, for the ith area can be expressed as:

$$u_i(s) = -\mathrm{TF_{PID}} \times e_i(t) \quad (6)$$

Differential Evolution Algorithm

The DE method is a parallel direct search method where N_p, D-dimensional parameter vector, is made use of as population for each iteration G. The algorithm is implemented to minimize the objective function defined in terms of $\Delta f_1, \Delta f_2$ and $\Delta P_{\mathrm{tie12}}$. During the process of minimization, the number of population members (N_P) remains constant. The initial vector population is chosen randomly covering the entire parameter space. As s set procedure, uniform probability distribution is assumed for all random decisions. In case the preliminary solution is available, the initial population might be generated by adding normally distributed random deviations to the nominal solution $x_{\mathrm{nom,o}}$. New parameter vectors are generated by adding the weighted difference of two population vectors to a third vector which is termed as mutation. Trial vector is generated by the crossover operation. If the fitness value of the trial vector turns out to be better than the target vector, then the trial vector is replaced by target vector. Details of the DE's basic strategy can be referred from [33, 34].

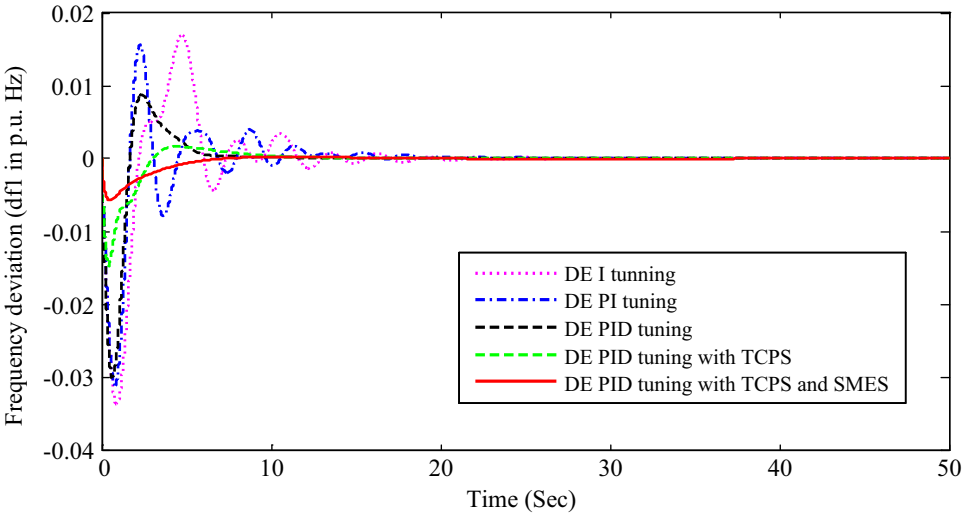

Fig. 7 Frequency deviation of area 1 versus time

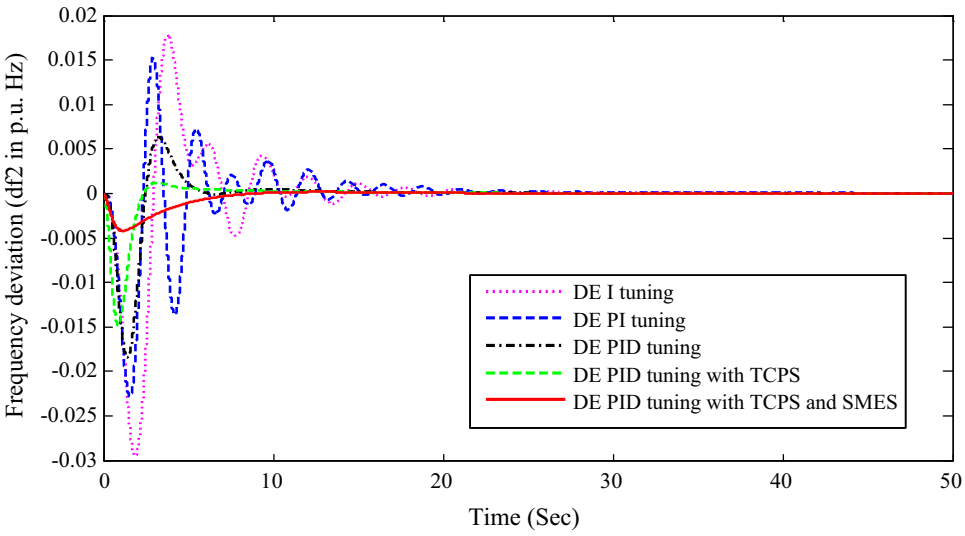

Fig. 8 Frequency deviation of area 2 versus time

Mutation

A mutant vector is generated for each target vector $X_{i,G} = 1, 2, 3, \ldots, N_p$ as follows:

$$V_{i,G+1} = X_{r_1,g} + F \cdot \left(X_{r_2,G} - X_{r_3,G}\right)$$

where r_1, r_2 and r_3 are random indices that belong to $\{1, 2, \ldots, N_P\}$, having integer values, and are mutually different with $F > 0$. The integers $r_1, r_2$and r_3 are also selected different from the running index i, so that N_P is greater than or equal to four to permit for this condition. F is a real and constant factor that belongs to [0, 2] which regulates the amplification of differential variation.

Crossover

To increase the diversity of the perturbed parameter vectors, the crossover operation is implemented and to achieve this, the trial vector is formed as follows:

$$U_{i,G+1} = (U_{1i,G+1}, U_{2i,G+1}, \ldots, U_{Di,G+1})$$

where

$$U_{ji,G+1} = \begin{cases} V_{ji,G+1}, & \text{if rand} \leq \text{CR or j} = I \\ X_{ji,G+1}, & \text{if rand} > \text{CR or j} \neq I \end{cases} \quad j = 1, 2 \ldots, D$$

Initialization

In this process, the upper bound X_j^U and lower bound X_j^L are defined for each parameter and the initial values of these bounds are selected randomly and uniformly.

Selection

After comparison of the target vector $X_{i,G}$ with the trial vector $V_{i,G+1}$, the one which is having lower function value goes to the next generation as mathematically explained below.

$$X_{i,G+1} = \begin{cases} V_{i,G+1}, & \text{iff}\left(V_{i,G+1}\right) < f\left(X_{i,G}\right) \\ X_{i,G}, & \text{otherwise} \end{cases}$$

where $i \in [1, N_P]$.

The operations of mutation, recombination and selection are continued until some terminating condition is reached.

Implementation of DE

While implementing the DE algorithm, certain fundamental parameters like mutation strategy, DE step size function also called scaling factor (F), crossover probability (CR), the number of population (NP), initialization, termination and evaluation function need to be decided. The value of F is usually in the range (0, 2) and controls the extent of perturbation in the mutation process. Crossover probability (CR) constants are generally selected between the interval (0, 1). The parameters used in this work for implementing the algorithm are as follows:

Number of population members (N_P) = 30
DE scaling factor (F) = 0.1
Crossover probability constant (CR) = 0.1
Maximum number of iterations of generations = 50
Lower bounds $(X_j^L) = [0\,0\,0 \ldots D]$
Upper bounds $(X_j^U) = [1.5\,1.5\,1.5 \ldots D]$

Results and Discussion

The LFC performance of the system shown in Fig. 1 is investigated under the effect of step load disturbance in area 1. The gain parameters of conventional PID controller and its variants, TCPS and SMES are optimized by DE

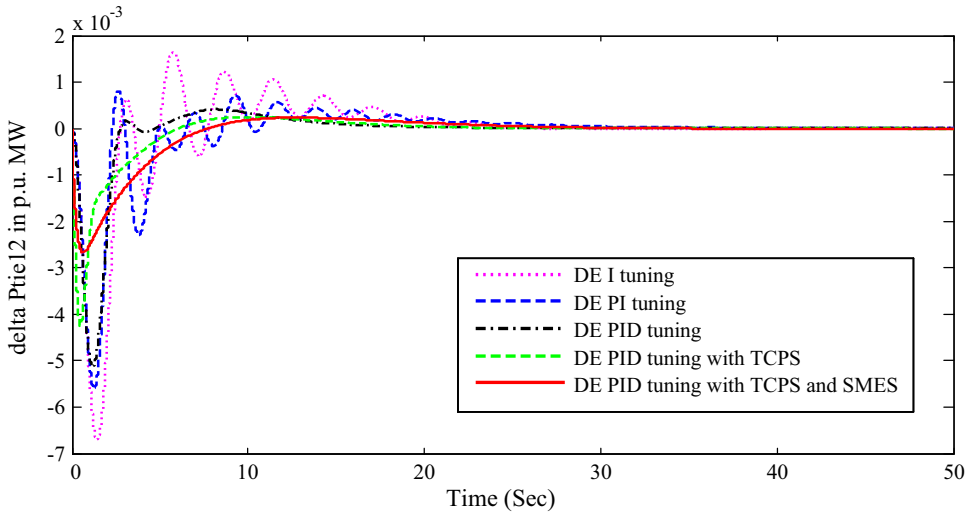

Fig. 9 Tie-line power deviation versus time

algorithm. Sensitivity analysis is also carried out with variations of system parameters and load. Simulations are carried out in MATLAB/Simulink environment. The simulations results are discussed under the following case study:

Case Study II: Without DFIG

In this case, the system of Fig. 1 is considered without DFIG. The conventional I/PI/PID controllers, optimized by DE algorithm, are implemented for each source in both areas, and the LFC performance is investigated under the impact of a step load change of 1% in area 1 at $t = 0$ s. The impact of TCPS and SMES on LFC is also observed. The comparative performance is depicted in Figs. 7, 8 and 9 in terms of deviations of frequency in both areas and the tie-line power. The comparative analysis is presented quantitatively in Table 1, in respect of the standard performance measures, viz. settling times with 2% tolerance band, maximum overshoot and minimum values of the performance index.

It is established that in LFC study, the maximum overshoot is more significant than settling time. As is evident from the comparison of results, both TCPS and SMES have positive impact on the LFC performance. It can be observed from Figs. 7, 8 and 9 that the use of TCPS

Table 1 Comparative analysis of performance of case study I

Performance index	DE-I	DE-PI	DE-PID	DE-PID with TCPS	DE-PID with TCPS and SMES
ITAE	0.9801	0.8065	0.2324	0.2104	0.1898
Settling time (t_s)					
Δf_1	16.4524	15.8547	6.0090	9.6830	13.6819
Δf_2	17.9704	21.1979	11.1460	8.9097	15.5353
ΔP_{tie}	20.8326	23.4838	14.8060	16.5697	20.2288
Maximum over shoot (M_P)					
Δf_1	0.0338	0.0313	0.0226	0.0147	0.0057
Δf_2	0.0295	0.0228	0.0137	0.0148	0.0042
ΔP_{tie12}	0.0067	0.0056	0.0038	0.0043	0.0027
Controller parameter					
Area 1					
Thermal					
K_P	–	0.4500	0.0559	0.8262	1.3431
K_I	0.3806	0.5102	1.4637	1.3064	0.8738
K_D	–	–	0.7835	0.0634	0.8741
Hydro					
K_P	–	1.3784	1.3644	1.3571	1.2824
K_I	1.4288	0.6844	0.5749	0.1965	0.0523
K_D	–	–	1.3267	1.2506	1.3281
TCPS					
K_{SMES}	–	–	–	0.5752	0.2545
SMES					
K_{TCPS}	–	–	–	–	0.3242
Area-2					
Thermal					
K_P	–	0.6837 s	0.3825	1.2007	0.6116
K_I	0.4473	0.6813	1.3636	1.3768	0.0546
K_D	–	–	1.3418	0.2060	1.1192
Hydro					
K_P	–	1.4179	0.5978	0.7571	0.2322
K_I	0.2376	0.3287	0.9375	0.6074	0.2159
K_D	–	–	0.8515	0.2604	0.9089
SMES					
K_{SMES}	–	–	–	–	0.4018

successfully improves the performance. However, the synergetic use of TCPS and SMES improves the LFC performance further, as is visible in the dynamic response of area frequencies and tie-line power exchanges, even without DFIG. For the situations without TCPS and SMES,

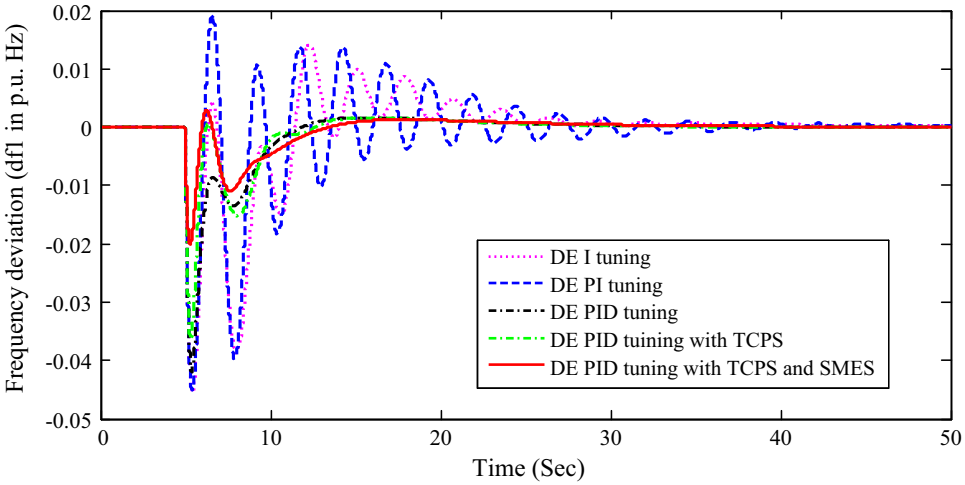

Fig. 10 Frequency deviation of area 1 versus time

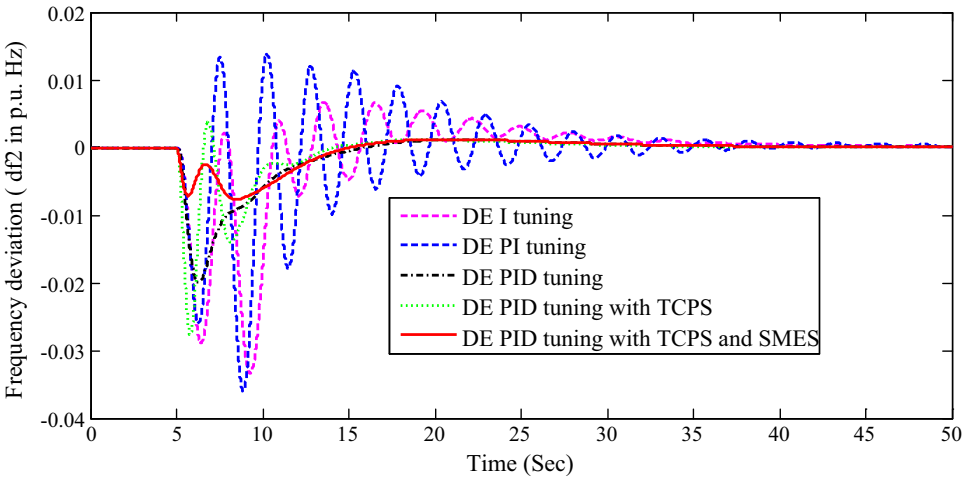

Fig. 11 Frequency deviation of area 2 versus time

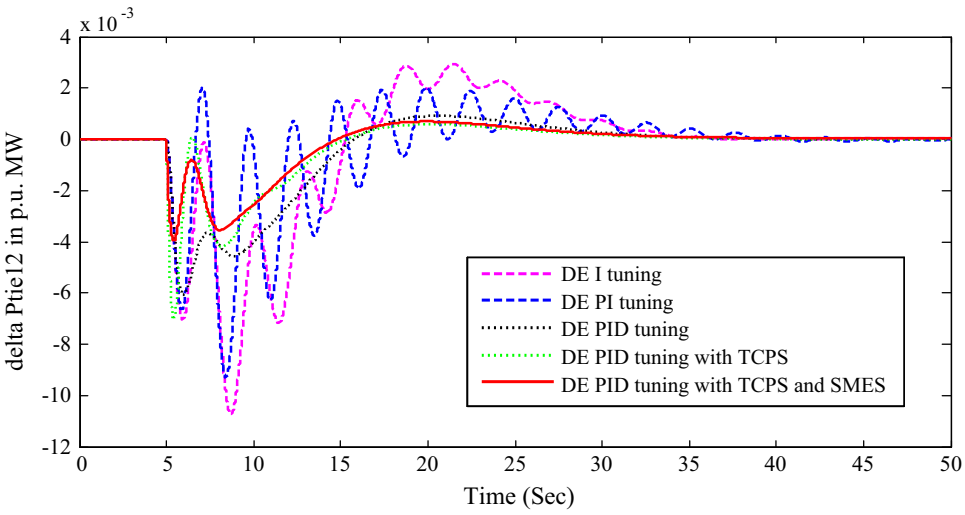

Fig. 12 Tie-line power deviation versus time

Table 2 Comparative analysis of performance of case study II

Performance index	DE-I	DE-PI	DE-PID	DE-PID with TCPS	DE-PID with TCPS and SMES
ITAE	5.4269	5.5841	2.4260	0.2104	0.1898
Settling time (t_s)					
Δf_1	29.5482	36.1482	22.5869	24.3784	25.2265
Δf_2	34.2053	38.4798	31.3223	20.4791	33.4736
ΔP_{tie}	33.1685	38.0970	33.0164	26.3029	30.7462
Maximum over shoot (M_P)					
Δf_1	0.0456	0.0451	0.0419	0.0336	0.0075
Δf_2	0.0334	0.0321	0.0277	0.0190	0.0088
ΔP_{tie12}	0.0107	0.0093	0.0061	0.0050	0.0071
Controller parameter					
Area 1					
Thermal					
K_P	–	0.3697	0.8636	0.1465	0.3057
K_I	0.4911	0.9911	1.285	1.3625	1.4900
K_D	–	–	0.7496	0.1620	0.1404
Hydro					
K_P	–	0.4941	0.6585	0.7755	0.9759
K_I	1.1190	0.9892	0.2236	0.2147	0.3228
K_D	–	–	0.0424	0.8391	0.3658
TCPS					
K_{TCPS}	–	–	–	0.2714	0.6065
SMES					
K_{SMES}	–	–	–	–	0.4015
Area 2					
Thermal					
K_P	–	0.0195	1.1350	0.0069	0.5095
K_I	1.1195	1.0771	1.1942	1.1500	0.2968
K_D	–	–	0.4403	1.2731	0.7603
Hydro					
K_P	–	0.5867	0.1728	1.3752	1.4261
K_I	0.2609	0.0503	0.5626	0.9870	0.5919
K_D	–	–	1.2433	0.5051	0.8767
SMES					
K_{SMES}	–	–	–	–	0.7146

the DE-tuned PID controller excels in performance as compared to other controller variants.

Case Study III: With DFIG

For this study, a test model is developed by connecting DFIG-based variable wind turbine to area 1 of the hydrothermal multi-source two-area power system. The dynamic modeling of DFIG was implemented as shown in Fig. 6. The parameters of DFIG are adapted from [5] and are given in Appendix with their usual meanings. The conventional I/PI/PID controllers, optimized by DE algorithm, are implemented for each source in both areas, and the LFC performance is investigated. The simulation study is carried out for small perturbation of 0.01 pu. in the wind speed, i.e., $\Delta\omega = 0.01$, applied to wind turbine at $t = 5$ s and 0.01 pu step load demand rise in area 1 applied at $t = 5$ s.

The impact of TCPS and SMES on LFC is also observed. The comparative performance is depicted in Figs. 10, 11 and 12 in terms of deviations of frequency in both areas and the tie-line power. The comparative analysis is presented quantitatively in Table 2, in respect of the standard performance measures, viz. settling times with 2%

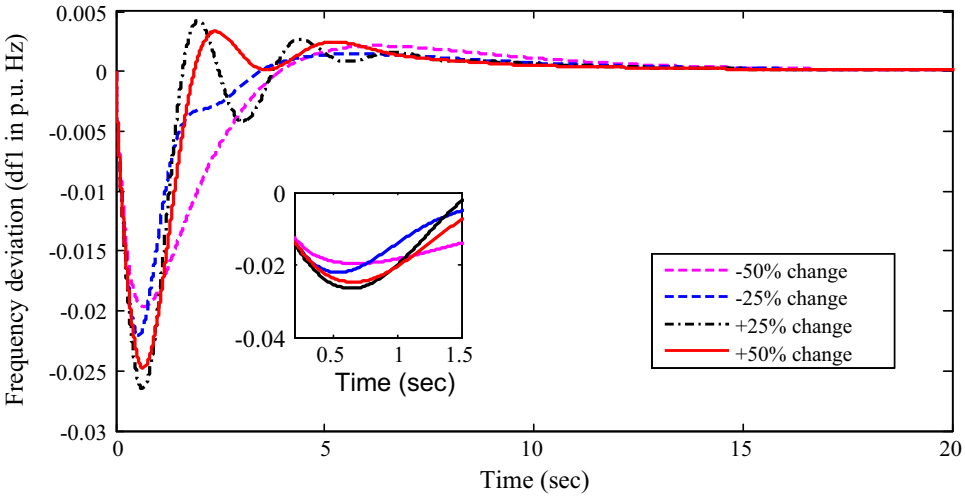

Fig. 13 Frequency deviations of area 1 with change in turbine time constants T_t and T_w

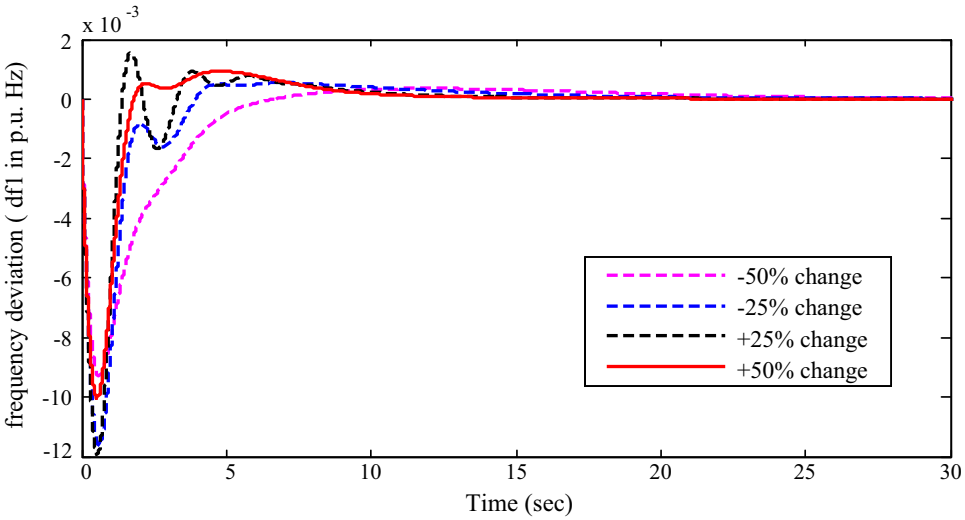

Fig. 14 Frequency deviations of area 1 with change in frequency bias B

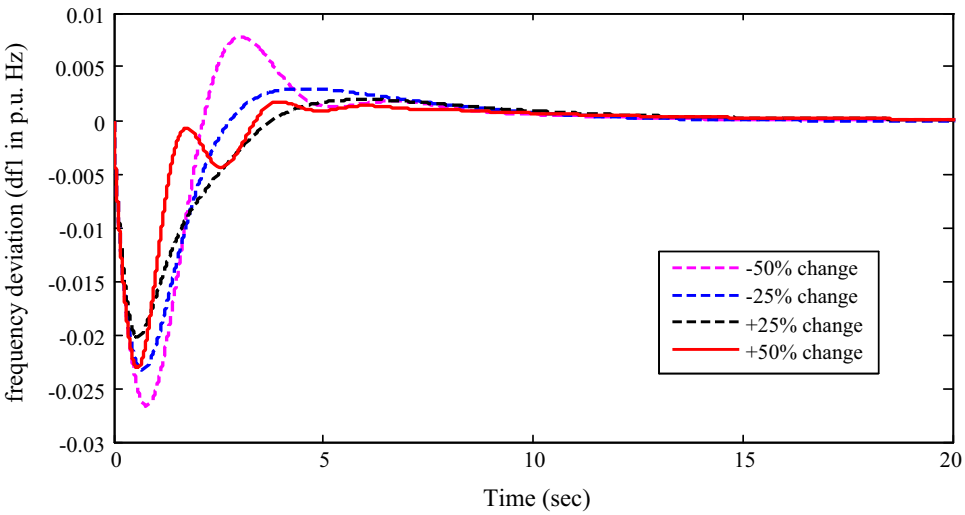

Fig. 15 Frequency deviation of area 1 with change in tie-line power coefficient T_{12}

tolerance band, maximum overshoot and minimum values of the performance index.

As is clear from Figs. 10 and 12, the positive impact of DFIG on the system frequency regulation is clearly

Table 3 Sensitivity analysis of multi-source hydrothermal power system

Parameters	Δf_1		Δf_2		ΔP_{tie12}	
	Settling time	Maximum overshoot	Settling time	Maximum overshoot	Settling time	Maximum overshoot
B						
− 50%	11.2710	0.0093	17.7257	0.0070	15.5048	0.0025
− 25%	10.3015	0.0116	16.7257	0.0066	15.6478	0.0029
25%	9.9328	0.0119	15.3573	0.0064	16.9514	0.0028
50%	9.6635	0.0100	15.5866	0.0055	18.0689	0.0024
T_{12}						
− 50%	10.1445	0.0266	14.5386	0.0127	17.4663	0.0053
− 25%	11.0483	0.0233	13.7957	0.0137	18.9140	0.0056
25%	12.0281	0.0202	16.2547	0.0150	17.3011	0.0059
50%	11.7546	0.0231	14.8115	0.0161	15.4624	0.0069
T_t and T_w						
− 50%	11.8681	0.0196	16.7403	0.0132	18.4727	0.0056
− 25%	10.0379	0.0221	16.6636	0.0123	17.1253	0.0053
25%	10.3752	0.0265	15.5739	0.0174	16.1322	0.0067
50%	9.9091	0.0248	15.0246	0.0144	15.7625	0.0063
SLD						
1%	17.1904	0.0153	16.8755	0.0184	16.8236	0.0063
5%	17.1122	0.0868	17.1452	0.1083	16.8699	0.0369
10%	22.4659	0.1749	15.9637	0.2128	18.2808	0.0727
15%	24.1509	0.2825	22.8403	0.3727	20.5984	0.1172
20%	24.5752	0.3632	22.6833	0.4602	33.2248	0.1501

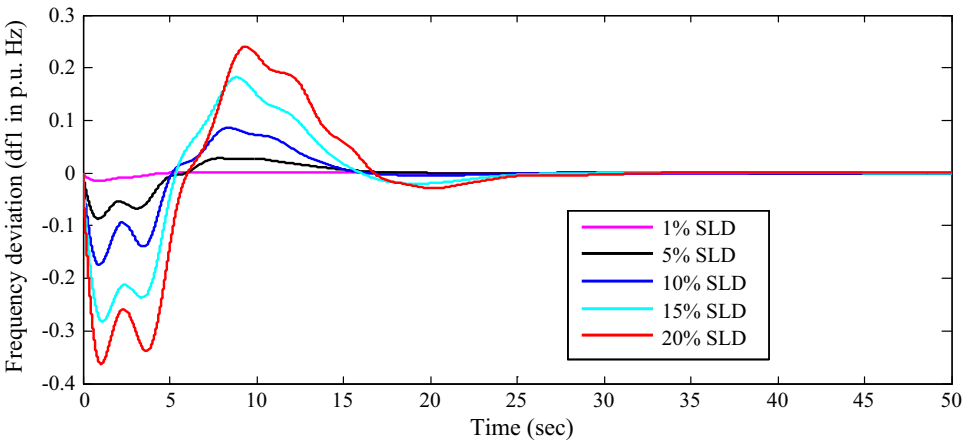

Fig. 16 Frequency deviation of area 1 for 1–20% SLD change in area 1

reflected and significant improvement in area frequency responses of both areas can be seen with DFIG providing active power support coupled with coordinated control of TCPS–SMES. Further, it is observed that frequency oscillations due to change in wind speed and load are damped out more quickly when TCPS and SMES are there in the system. For different situations with or without TCPS and SMES, the DE-tuned PID controller excels in performance as compared to other controller variants

Case Study IV: Sensitivity Analysis

Simulations are carried out for sensitivity study to assess the robustness of the control performance of the system of Fig. 1, considered without DFIG, TCPS and SMES, to wide changes in the operating conditions and system parameters. The system is subjected to changes, taking one at a time, in operating load condition and time constants T_t and T_w of turbines, frequency bias coefficient and tie-line

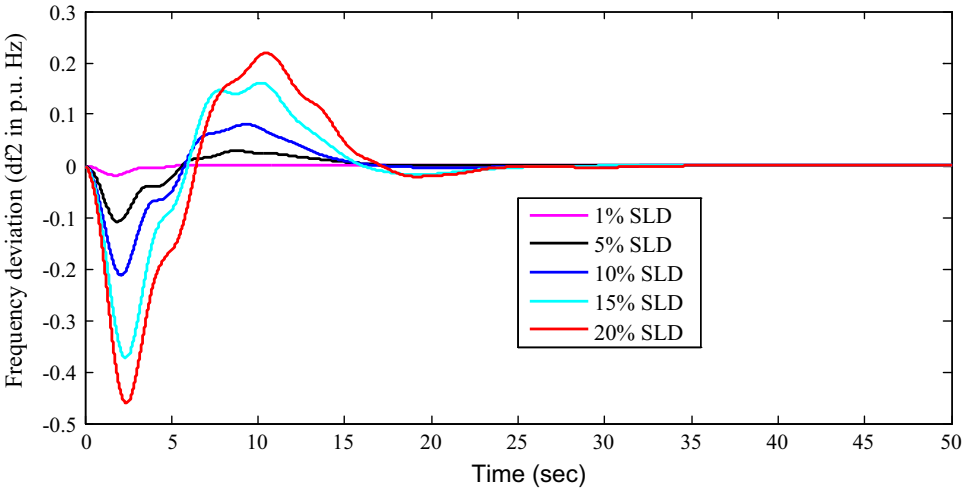

Fig. 17 Frequency deviation of area 2 for 1–20% SLD change in area 1

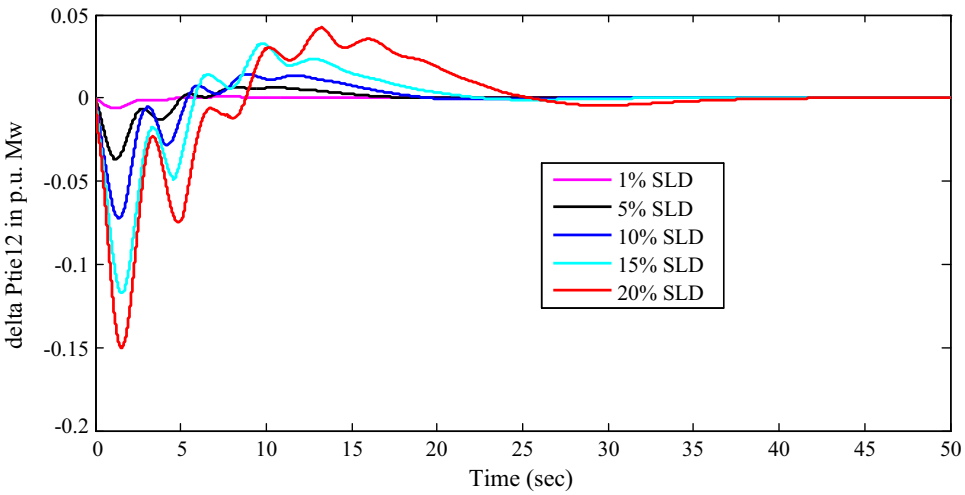

Fig. 18 Tie-line power deviation for 1–20% SLD change in area 1

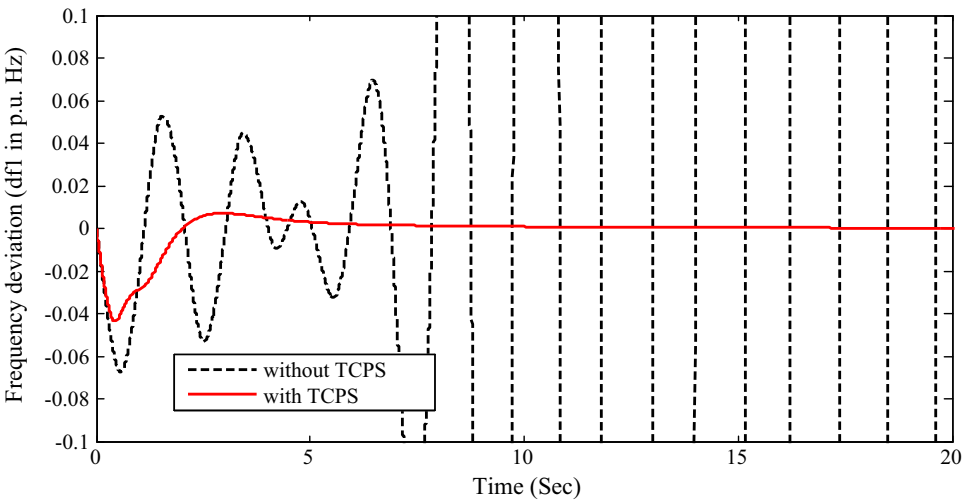

Fig. 19 Frequency deviation of area 1 with change in inertia constant

power coefficient T_{12} from their nominal values (given in "Appendix") in the range of ± 50% in steps of 25%. These changes are effected in both areas simultaneously. The PID controller, optimized using DE algorithm employing ITAE objective function, is implemented with all variations for sensitivity analysis. Figures 13, 14 and 15 depict the effect

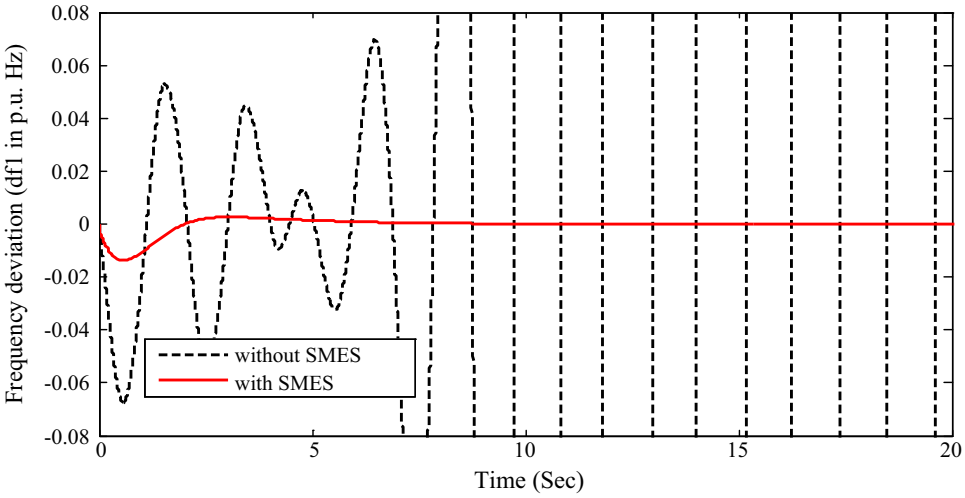

Fig. 20 Frequency deviation of area 1 with change in inertia constant

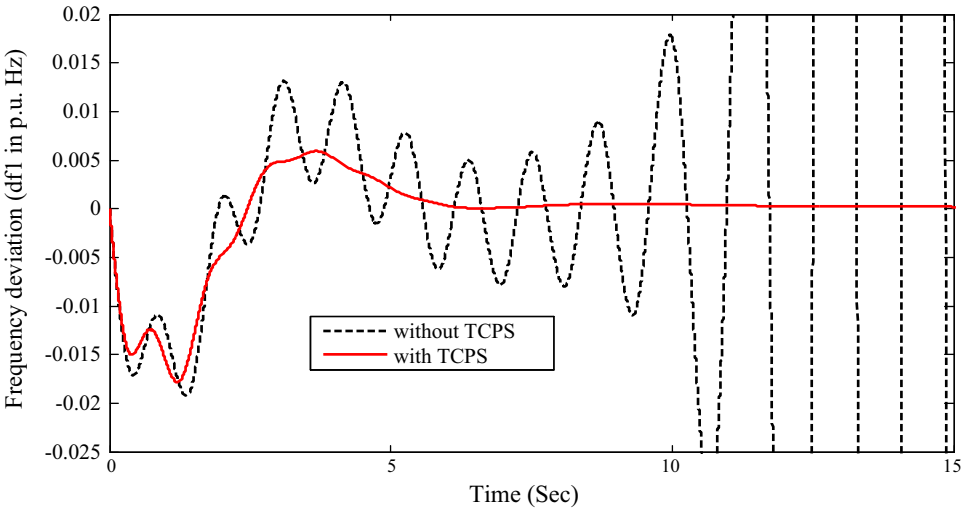

Fig. 21 Frequency deviation of area 1 with change in tie-line

of variation of system parameters on the frequency deviation of area 1. The quantitative analysis of the performance is reflected in the values of the performance measures, i.e., settling time and peak overshoot, as given in Table 3. It can be observed from Figs. 13, 14 and 15 and Table 3 that the effect of the variation of system parameters on the system performance is negligible. Therefore, it can be inferred that the proposed control strategy provides robust solution.

To study the robustness of the proposed control scheme, i.e., PID controller tuned by DE algorithm, against variations in step load disturbance (SLD), the system of Fig. 1 is considered with TCPS and SMES both connected and the SLD is changed in the range of 1–20% with a step size of 5%. PID controllers used in both areas are optimally tuned by DE algorithm for all loading conditions separately. The dynamic responses are shown in Figs. 16, 17 and 18. It is evident from Figs. 16, 17 and 18 that with the variation of loading conditions, there is negligible effect on the frequency deviation response with the proposed control scheme and the power system behavior is robust against changes in load.

Case Study V: Weak Grid

To establish the validity of the proposed control approach under wide variations of the operating conditions, the case study was carried out for a weak grid condition also. For demonstrating the effectiveness of the DE-PID controller under weak grid condition, the main system (Fig. 1) parameters: inertia constant and tie-line constant, are significantly changed, one at a time, till the overall system becomes weak. Then, TCPS and SMES are connected, individually, in the system, to study their stabilizing effect on the frequency regulation. The closed-loop frequency responses, after applying these changes to the power system parameters, are shown in Figs. 19, 20 and 21, respectively. It can be seen from Figs. 19, 20 and 21 that without TCPS and SMES system cannot handle the applied

parameters' perturbation, whereas due to the participation of TCPS and SMES in the frequency control, the initial drop as well as other frequency deviations are reduced.

Conclusion

This paper implemented the DE algorithm-tuned conventional controllers to study the LFC performance of a two-area multi-source hydrothermal power system having penetration of DFIG in one of the areas. Besides analyzing the impact of dynamic active power support from DFIG on the frequency control, the paper has also analyzed the impact of TCPS and SMES on the system performance under wide variations in the operating conditions, including the weak grid condition. The gain parameters of TCPS and SMES were also tuned using DE algorithm, besides the controller gain parameters. It is established that TCPS, when used in coordination with SMES, improves the performance substantially coupled with the positive impact of DFIG. The performance is analyzed qualitatively as well as quantitatively in respect of different performance parameters. Robustness analysis of the DE-PID controller for the multi-source two-area hydrothermal power system is also carried out by varying different parameters, considered one at a time, of both the areas simultaneously in the range of $\pm$ 50% of the nominal value, in steps of 25%, besides varying the SLD from 1 to 20% of nominal value, in steps of 5%. Qualitative and quantitative analyses of simulation results reveal that DE-PID controllers are robust under wide variations in system parameters and loading conditions. The improved simulation results are encouraging and indicative of the potential application of the DE algorithm-tuned control schemes to the LFC studies in power systems integrated with wind power.

Appendix: System Parameters [5, 10, 11, 16]

System parameters	Description	Values used in this work
F	Nominal system frequency	60 Hz
I	Subscript referring to area	i = 1,2
K_{Pi}	Power system gain	120 Hz/p.u. MW
T_{Pi}	Power system time constant	20 s
R_i	Regulation droop	2.4 Hz/p.u. MW
B_i	Frequency biasing coefficient	0.425 p.u. MW/Hz
T_{12}	Tie-line synchronizing coefficient	0.0466
Reheat thermal		
T_g	Time constant of governor	0.08 s
T_t	Turbine time constant	0.3 s
T_r	Reheat time constant	10
K_r	Reheat coefficient	0.5
GRC	Generation rate constant	4%/min
Hydro		
T_R	Hydro-governor time constant	5
T_{TH}	Steam chest time constant	41.6
T_{GH}	Hydro-governor time constant	0.513
T_w	Water starting time	1 s
GRC	Generation rate constraint	270%/min (raising generation)
		360%/min (lowering generation)
TCPS parameters		
φ_{max}	Phase shifter max limit	10°
φ_{min}	Phase shifter min limit	−10°
T_{PS}	TCPS time constant	0.01
SMES parameters		
T_1	SMES time constant	0.2333
T_2	SMES time constant	0.016
T_3	SMES time constant	0.7087
T_4	SMES time constant	0.2481
T_{SMES}	SMES time constant	0.03
DFIG parameters		
H_e	Wind turbine inertia	3.5 p.u MW. s
K_{wp}	DFIG proportional speed controller gain	1
K_{wi}	DFIG integral controller gain	0.1
T_r	Transducer time constant	15 s
T_w	Washout filter time constant	6 s
T_a	DFIG turbine	0.2 s

References

1. J. Ekanayake, N. Jenkins, Comparison of the response of doubly fed and fixed-speed induction generator wind turbines to change in network frequency. IEEE Trans. Energy Convers. **19**(4), 800–802 (2004)
2. G. Lalor, J. Ritche, S. Rourke, D. Flynn, M. O'Malley, Dynamic frequency control with increasing wind generation, in *Proceedings of the IEEE Power Engineering Society General Meeting, Denver, CO*, pp. 6–10 (2004)
3. X. Yingcheng, T. Nengling, Review of contribution to frequency control through variable speed wind turbine. Renew Energy **36**, 1671–1677 (2010)

4. J. De'Almeida, R.G. Lopes, Participation of doubly fed induction wind generators in system frequency regulation. IEEE Trans. Power Syst. **22**(3), 944–950 (2007)
5. A. Kumar, Sathans, Impact study of DFIG based wind power penetration on LFC of a multi-area power system, in IEEE Conference (2015)
6. J. Morren, S.W.H. Haan, W.H. Kling, J.A. Ferreira, Wind turbines emulating inertia and supporting primary frequency control. IEEE Trans. Power Syst. **21**(1), 433–434 (2006)
7. P. Keung, P. Lei, H. Banakar, B.T. Ooi, Kinetic energy of wind-turbine generators for system frequency support. IEEE Trans. Power Syst. **24**(1), 279–287 (2009)
8. M. Kayikci, J.V. Milanovic, Dynamic contribution of DFIG-based wind plants to system frequency disturbances. IEEE Trans. Power Syst. **24**(2), 859–867 (2009)
9. S.C. Tripathy, R. Balasubramanian, N.P.S. Chandramohanan, Effect of superconducting magnetic energy storage on automatic generation control considering governor dead band and boiler dynamics. IEEE Trans. Power Syst. **7**(3), 1266–1273 (1992)
10. Y. Mitani, K. Tsuji, Y. Murakami, Application of superconducting magnetic energy storage to improve power system dynamic performance. IEEE Trans. Power Syst. **3**(4), 1418–1425 (1988)
11. J.A. Rajesh, D. Das, A. Patra, AGC of a hydrothermal system with thyristor controlled phase shifter in the tie-line, in IEEE Power India Conference (2006)
12. N.G. Hingorani, L. Gyugyi, *Understanding FACTS* (Concepts and Technology of Flexible Ac Transmission System. IEEE Press, New York, 2000)
13. N. Ibraheem, P. Kumar, D.P. Kothari, Recent philosophies of automatic generation control strategies in power systems. IEEE Trans. Power Syst. **20**(1), 346–357 (2005)
14. S.K. Pandey, S.R. Mohanty, N. Kishor, A literature survey on load-frequency control for conventional and distribution generation power systems. Renew. Sustain. Energy Rev. **25**, 318–334 (2013)
15. K.P.S. Parmar, S. Majhi, D.P. Kothari, Load frequency control of a realistic power system with multi-source power generation. Int. J. Electr. Power Energy Syst. **42**, 426–433 (2012)
16. J. Nanda, A. Mangla, S. Suri, Some new findings on automatic generation control of an interconnected hydrothermal system with conventional controls. IEEE Trans. Energy Convers. **21**(1), 187–194 (2006)
17. P. Melin, L. Astudillo, O. Castillo, F. Valdez, M. Garcia, Optimal design of type-2 and type-1 fuzzy tracking controllers for autonomous mobile robots under perturbed torques using a new chemical optimization paradigm. Expert Syst. Appl. **40**(8), 3185–3195 (2013)
18. S.P. Ghoshal, Application of GA/GA-SA based fuzzy automatic generation control of a multi area thermal generating system. Electr. Power Syst. Res. **70**, 115–127 (2004)
19. H. Gozde, M.C. Taplamacioglu, Automatic generation control application with craziness based particle swarm optimization in a thermal power system. Int. J. Electr. Power Energy Syst. **33**, 8–16 (2011)
20. A.M. Jadhav, K. Vadirajacharya, E.T. Toppo, Application of particle swarm optimization in load frequency control of interconnected thermal-hydro power systems. Int. J. Swarm Intell. **1**(1), 91–112 (2013)
21. E.S. Ali, S.M. Abd-Elazim, Bacteria foraging optimization algorithm based load frequency controller for interconnected power system. Int. J. Electr. Power Energy Syst. **33**, 633–638 (2011)
22. S. Panda, B. Mohanty, P.K. Hota, Hybrid BFOA-PSO algorithm for automatic generation control of linear and nonlinear interconnected power systems. Appl. Soft Comput. **13**, 4718–4730 (2013)
23. L.C. Saikia, S. Mishra, N. Sinha, J. Nanda, Automatic generation control of a multi area hydrothermal system using reinforced learning neural network controller. Int. J. Electr. Power Energy Syst. **33**(4), 1101–1108 (2011)
24. R. Elyas, Intelligent linear-quadratic optimal output feedback regulator for a deregulated automatic generation control system. Electr. Power Compon. Syst. **40**(5), 513–533 (2013)
25. P. Ibraheem, K.N. Hasan, N. Nizamuddin, Suboptimal automatic generation control of interconnected power system using output vector feedback control strategy. Electr. Power Componen. Syst. **40**(9), 977–994 (2012)
26. D.K. Chaturvedi, P.S. Satsangi, P.K. Kalra, Load frequency control: a generalized neural network approach. Electr Power Energy Syst. **21**, 405–415 (1999)
27. R.K. Sahu, S. Panda, S. Padhan, A novel hybrid gravitational search and pattern search algorithm for load frequency control of nonlinear power system. Appl. Soft Comput. **29**, 310–327 (2015)
28. P.C. Pradhan, R.K. Sahu, S. Panda, Firefly algorithm optimized fuzzy PID controller for AGC of multi-area multi-source power systems with UPFC and SMES. Eng. Sci. Technol. Int. J. **16**, 338–354 (2016)
29. B.K. Sahu, S. Pati, P.K. Mohanty, S. Panda, Teaching–learning based optimization algorithm based fuzzy-PID controller for automatic generation control of multi-area power system. Appl. Soft Comput. **27**, 240–249 (2015)
30. B.K. Sahu, T.K. Pati, J.R. Nayak, S. Panda, S.K. Kar, A novel hybrid LUS–TLBO optimized fuzzy-PID controller for load frequency control of multi-source power system. Electr. Power Energy Syst. **47**, 58–69 (2016)
31. R.B. Chedid, S.H. Karaki, C. El-Chamali, Adaptive fuzzy control for wind-diesel weak power systems. IEEE Trans. Energy Convers. **15**(1), 71–78 (2000)
32. M.F.M. Arani, Y.A.R.I. Mohamed, Analysis and impacts of implementing droop control in DFIG-Based wind turbineson microgrid/weak-grid stability. IEEE Trans. Power Syst. **30**(1), 385–396 (2015)
33. S. Das, P.N. Suganthan, Differential evolution: a survey of the state-of-the-art. IEEE Trans. Evol. Comput. **15**, 4–31 (2011)
34. S. Panda, Robust coordinated design of multiple and multi-type damping controller using differential evolution algorithm. Int. J. Electr. Power Energy Syst. **33**, 1018–1030 (2011)